

Hierarchical Matching and Regression with Application to Photometric Redshift Estimation

Fionn Murtagh
email: fmurtagh@acm.org

May 26, 2022

Abstract

This work emphasizes that heterogeneity, diversity, discontinuity, and discreteness in data is to be exploited in classification and regression problems. A global *a priori* model may not be desirable. For data analytics in cosmology, this is motivated by the variety of cosmological objects such as elliptical, spiral, active, and merging galaxies at a wide range of redshifts. Our aim is matching and similarity-based analytics that takes account of discrete relationships in the data. The information structure of the data is represented by a hierarchy or tree where the branch structure, rather than just the proximity, is important. The representation is related to p -adic number theory. The clustering or binning of the data values, related to the precision of the measurements, has a central role in this methodology. If used for regression, our approach is a method of cluster-wise regression, generalizing nearest neighbour regression. Both to exemplify this analytics approach, and to demonstrate computational benefits, we address the well-known photometric redshift or ‘photo-z’ problem, seeking to match Sloan Digital Sky Survey (SDSS) spectroscopic and photometric redshifts.

Keywords: Cluster-wise regression, p -adic and m -adic number representation, inherent hierarchical properties of data

1 General Introduction

We are concerned with matching, and drawing inferences (extrapolation and interpolation, prediction, distributional degree of association, etc.) from structures that are discrete. In addition to being discrete, there are associations, similarities and identities that are relevant. Also relevant are incorporation, inclusion, properties of an object being a subset of properties of one or more other objects.

A reasonable and a natural representation for such structures is an ultrametric or tree topology. Our objects are taken as nodes of a tree. A tree is a synonym for hierarchy. These objects, or entities, could, if desired, include sub-objects and sub-entities also. In set notation, a hierarchy is a partially ordered

set, or poset: let sets q, q' , associated with nodes, have a least common parent node, q'' . Parent/child node ordering uses $q, q' \subset q''$. For a partially ordered set, it is required that for any two subsets. $q, q' \in 2^I$, for power set 2^I where I is the union of all sets, or the universal set: one class is a subset of the other, as the only permitted overlapping: $q \cap q' = \emptyset$ or either $q \subset q'$, or $q' \subset q$.

2 Real Number System: Practicalities of p-Adic and m-Adic Number Systems

In our Baire, longest common prefix, metric, from which we can directly (i.e. in linear computational time) read off a hierarchy, we must explain why the resulting clusters are meaningful in the following sense: why is it reasonable to have different clusters, from the top or first level or partition onwards, for 2.9999 and 3.000, for example?

Firstly, our approach assumes precise measurement to a given precision. Our Baire method favours contexts where the digits of precision of measurement are ordered (decreasing importance associated with increasing digit of precision). Hence our Baire methodology is designed for fast, exact proximity matching.

So – tree branch is what is important here, rather than just the proximity, alone, of singletons. We might even say, if the singletons are derived from, or originate from, the root, then precisely how they came about from the root, i.e. their path from the root, that is what we want to especially take into consideration. In this very particular sense then, we have that 0.50 is distinct from 0.49, and, we reason further, 0.500 is distinct from 0.499, and so on, just due to the account taken of digit priority.

A further perspective on this, and justification for the role of digit sequence, is as follows. Consider that we are measuring with these two exemplary numbers here, and what we additionally want to do is to “take time into account”, with time steps, say milli-seconds, being used for determining each additional digit in what we are measuring. We are determining our numbers, digit by digit. In each such digit stage, or, informally expressed, in each such “time-step”, we are adding detail and precision to our measured values.

Of course it is to be accepted that in a real number system, by convention a p-adic number system when $p = \infty$, 0.5 is identical to, and can be expressed as 0.499999.... Irrespective of whether taking real numbers as an m-adic number system, with $m = 10$, or, with their important mathematical properties, considering p-adic number systems, for p prime, our concluding remark is as follows. We take into consideration a priority order of digits.

One further example of this adic number representation is as follows. In [8], the dynamics of fluid flows in tree branchings is at issue. This is with application to petroleum underground reservoirs.

3 Previous Work

3.1 Determining Photometric Redshifts from Colour and Magnitude Observed Data, and Evaluating relative to Spectroscopic Redshifts

In [16] there is predicting of photometric redshifts “from an ultra deep multicolor catalog”. Training is carried out with spectroscopic redshifts. This is noted: “the difficulty in obtaining spectroscopic redshifts of faint objects”, and then: “A crucial test in all cases is the comparison between the photometric and spectroscopic redshifts which is typically limited to a subsample of relatively bright objects”. The SDSS DR1 catalogue used is “almost entirely limited to $z < 0.4$ ”. The test sample is 88108 galaxies, and 24892 galaxies in the training sample. It is noted how other approaches to nonlinear regression, including a Bayesian method, polynomial regression and nearest-neighbour regression are claimed to perform worse (citing [3]). The latter work, [3], uses approximately 35000 galaxies with spectroscopic redshifts, from the SDSS EDR (Early Data Release) database, pre-DR1 (Data Release 1, the most recent at the time of writing, being DR-12). In [3], $0.2 < z < 0.3$ redshifts are used. Colour and magnitude data are used to estimate photometric redshifts. In [7], a training set of 10000 and a test set of 7000 SDSS objects (galaxies but indicating that stars are also included, with $z < 0.5$).

3.2 Interval Measurements for Bayesian “stacking” Modelling; Accuracy and Correctness of Measurement

In [14] velocity distributions are at issue, for association with galaxy sizes, to “determine ‘dynamical masses’ that are independent of stellar-population assumptions”, with that to be used for evolution of galaxies for given mass, following relationship estimation with mass and gravitational potential. Interest is in elliptical galaxies, that are “To a first approximation ... ‘pressure-supported’ rather than rotationally supported”. Velocity dispersion is to be based on spectroscopic data. Now, in particular for faint, even if luminous, galaxies, there will be uncertainty and non-Gaussianity in measurement. From SDSS III, 430000 galaxies are used, primarily with redshifts $0.2 < z < 0.8$. Eigenspectra are determined from principal components analysis. Because of the imprecision of measurement the following is carried out, in the estimation of velocity dispersion. Both in redshift and in absolute magnitude, respectively with intervals of 0.04 and 0.1, galaxies are binned. Therefore, for error or imprecision of measurement, binning, i.e. interval measurements, are a way to somewhat robustify the data. Based on extensive analyses, it is concluded that here the “stacking” of multiple spectra is replaced by a new “Bayesian stacking” approach. (The hierarchical Bayesian approach is summarized in section 3.2 of [14]).

In [2], use is also made of the work of [14]. Under “Known issues”, there are the following: the use of probability priors on principal component analysis coefficient combinations; spectra that are obscured by others, e.g. quasar spectra,

by AGN spectra; spectra affected by “cross-talk from bright stars”; superpositioning of observed objects; and a few classes of object, and detector suitability (“fibers near the edge of the spectrograph camera fields of view”).

3.3 Nonlinear Regression

In [4], multilayer perceptrons (MLPs) are used to relate photometric redshifts to spectral information. Varying object classes (normal galaxies, stars, late type stars, nearby AGNs, distant AGNs) are subject to principal component analysis of spectra, to provide an eigenvector-based spectral classification index.

The case is then made for carrying out the nonlinear regression, using MLP, on two different redshift intervals, $z < 0.25$ and $z > 0.25$. Differing galaxy populations are associated with these redshift intervals. A total of 449370 galaxies were studied. Just interestingly, consideration was given to not too full redshift intervals used for training, but $[0.01, 0.25] \subset [0.0, 0.27]$ and $[0.25, 0.48] \subset [0.23, 0.50]$.

The foregoing work is pursued in [5]. SDSS DR4 data was used. A most comprehensive introduction is provided (section 1, Introduction, section 2, Photometric redshifts). Included is the following note: “photometric redshift samples are useful if the structure of the errors is well understood”, because this points to the reliability of, and confidence in, measurement. Later there are these statements: “photometric redshift estimates depend on the morphological type, age, metallicity, dust, etc. it has to be expected that if some morphological parameters are taken into account besides the magnitudes or colors alone, estimates of photometric redshifts should become more accurate.” In this work, the “near universe”, $z < 0.5$, is at issue, and also with discussion of “the near and intermediate redshift universe”, $z < 1$. As before, two separate MLPs were used on this data, for “nearby”, $z < 0.25$, and for “distant”, $z > 0.25$ objects. These objects comprised 449370 galaxies.

A most revealing statement is the following: “the derivation of photometric redshifts requires, besides an accurate evaluation of the errors, also the identification of a homogeneous sample of objects.”

4 Data Analysis

4.1 Data and Objectives To Be Pursued

SDSS (Sloan Digital Sky Survey) data used was from Data Release 5, [1], relating to the following: “Stripe 82 is an equatorial region repeatedly imaged during 2005, 2006, and 2007”, [15]. Data were as follows: number of objects: 443094; right ascension, declination, spectroscopic redshift, photometric redshift. Then minimum redshifts, respectively spectroscopic and photometric, are: 0.000100049, 0.0001035912, and the maximum redshifts are: 0.599886, 0.5961629.

Our objective is to assess spectroscopic redshift from photometric redshift. While regression, whether classical linear (statistical least squares), or nonlinear (multilayer perceptron, k-nearest neighbour, etc.) are relevant, we seek the following.

1. Take the discreteness of measurement into account.
2. Therefore, we take distinction of value to be primarily associated with the discrete sourcing of our measurements, rather than being solely a statistical uncertainty or error component of our measurement.
3. However statistical uncertainty or error component of measurement are taken as integral to the discreteness of sourced data.
4. It arises from this reasoning that what is important in practice is to be able to codify one's data, in the sense both of data encoding and of data representation, here related to number theory.
5. From the data encoding and representation, we are seeking to associate data interpretation and understanding, with the discrete sourcing of our measured data.

While cosmology presents the primary motivation for our m -adic and p -adic analytics, applications and opportunities for similar perspectives are numerous in other sciences also. (A small set of notes follow. Notationally $m > 2$ is typically a positive integer, and p is prime. An m -adic number system is a ring, while a p -adic number system constitutes a field. A field has a multiplicative inverse for non-zero values, i.e. it permits division.)

4.2 Preliminary Data Analysis

For initial exploratory analysis purposes, we consider the histograms, cf. Figure 1. While mainly peaked around the lower redshifts, there are some other interesting smaller peaks. The digits of precision of the data are at issue. It is to be noted that some data values are limited to about three digits of precision.

A first analysis will look at the very first digit of precision. From the 443094 objects, we find that a 0 first digit of precision is shared by 162034 spectroscopic and photometric redshifts; a 1 first digit of precision is common to 144602 redshifts; a 2 first digit of precision is common to 22643 redshifts; a 3 first digit of precision is common to 26441 redshifts; a 4 first digit of precision is common to 11166 redshifts; and a 5 first digit of precision is common to 21 redshifts. Overall, the first digit of precision of the spectroscopic and photometric redshifts is common to 366907 objects, that is, 83% of all cases.

This is encouraging to begin with. It indicates one relevant and useful way to determine commonality, or association, between the more reliable spectroscopic redshifts and the possibly more accessible photometric redshifts. The next stage of our analysis is to see if this finding, of 83% commonality of spectroscopic and photometric redshift measurement, can be furthered.

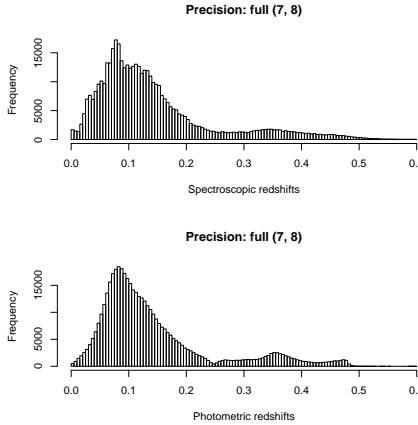


Figure 1: Full precisions, 7 or 8 digits. Top, spectroscopic, and bottom, photometric.

If we look at both the shared first digit of precision, and additionally a difference in the first digit of precision of at most 1, then we find that 99.6% of all the spectroscopic and photometric redshift measurement are that close in measurement value. While this is motivational, it requires further study of just what redshifts differ by 1 in the first digit of precision. However, we do not consider such a finding as generally and broadly applicable.

5 Re-Representing Our Data in p -Adic and Other Number Systems

5.1 Number Systems Other Than Real

In the regression-oriented matching of spectroscopic redshift and photometric redshift values, motivation for our approach is as follows.

With reference to the histograms displayed in the previous section, in 3-dimensional Euclidean space, assumed distribution functions could be used to calibrate one such distribution function against another. This “calibration” could be cluster-based, through determining, for example, a Gaussian mixture fit to the assumed distribution functions. Gaussian model-based mixtures can also be hierarchical, providing model-based cluster trees, [10]. Another viewpoint could be to use RA and Dec local dependencies. That could imply the regression of RA, Dec, z_s on z_p (the latter denoting spectroscopic redshift, photometric redshift).

Now, compared to a Euclidean and Hilbert space, we are dealing with discrete object locations and clustered, albeit delimited, regions of objects. A

graph and more particularly, a tree is an appropriate representation, rather than a continuous space. Although a side remark in the current context, it was noted in section 2 how an ordered time dimension, in particular through being ordered rather than being real-valued, can also be subsumed in this approach.

Because of the directly mapped, rooted tree representation that can be associated with any m -adic number representation, we proceed as follows: consider our given decimal or base 10 measurements, as m -adic with $m = 10$. Efficiently derive other m -adic number representations, to assess them.

5.2 Re-Representing Data in Other Number Systems, through Efficient Approximation

In [11], the following innovative approach was developed for re-representing a data set, represented m -adically by a closest fit approximation by a data set, represented $(m - 1)$ -adically.

For all neighbour or adjacent digit values, at a given precision level, that have the same parent digit value, i.e. at these digit values' immediate preceding precision level, assess the following. Firstly, if these neighbour values are identical, then there will be no intervention. Secondly, if these neighbour values differ by more than 1, then there will be no intervention. Thirdly, if these neighbour values differ by 1, then assessment is made of what overall pair of such values, with the same parent value, and differing by 1, are such that their cardinality is minimal. We are going to merge this set of neighbour values. The following properties of this processing are as follows. By design, this constitutes a minimal overall change in our data. This implies one digit less, in the entirety of data representation. Therefore this is a best approximation to our data, starting from an m -adic representation, and passing to an $m - 1$ -adic representation. There remains one final part of this processing: from the chosen set of neighbour digit values, the larger of these two values is altered to the smaller of these two values. That is carried out in the data. Very finally, for consistency and coherence of number representation, all values that were greater than this modified value are decreased by 1.

The effectiveness of this approach was demonstrated in [11]. Computationally it is linear in the numbers of objects multiplied by the number of digits of precision. That is, it is linear in the data set size, expressing the total number of digits.

5.3 m -Adic Fitting of Spectroscopic Redshifts

As described in the previous subsection, we fit the given m -adic data, for $m = 10$, with the best fitting $m = 9$ -adic representation; then with the (stepwise) best fitting $m = 8$ -adic representation; then with the (stepwise) best fitting $p = 7$ -adic representation; then with the (stepwise) best fitting $m = 6$ -adic representation; then with the (stepwise) best fitting $p = 5$ -adic representation; then with the (stepwise) best fitting $m = 4$ -adic representation; then with the

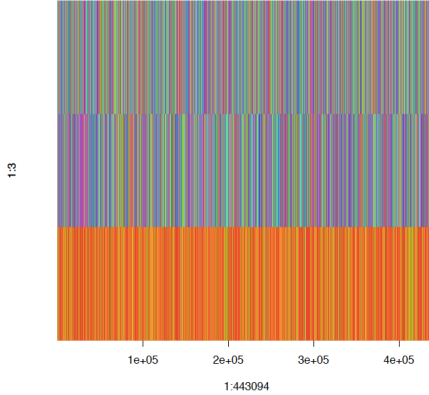


Figure 2: Spectroscopic redshifts. Initial m -adic display, for $m = 10$. Three digits of precision used, increasing on the ordinate. The abscissa lists the spectra.

(stepwise) best fitting $p = 3$ -adic, or ternary, representation; and finally with the (stepwise) best fitting $p = 2$ -adic, or binary, representation.

The outcomes are shown in the following figures. Since some of the redshift data values are just three digits in precision, that was the extent of data precision that was used. See Figures 2, 3.

In Figure 4 there is a plot of distances squared, i.e. squared error, between the original (m -adic, with $m = 10$) data and the other m -adic representations. Note that appropriate normalization (rescaling to $(0, 1)$ for each m -adic representation) precedes the calculation of distance squared.

A minor remark follows on Figure 4: the best p -adic fit to our data is the 7-adic representation.

5.4 m -Adic Fitting of Photometric Redshifts

As described in the previous subsection, for spectroscopic redshifts, we now study the photometric redshifts.

The outcomes are shown in the following figures. Three-digit data precision was used. See Figure 5.

In Figure 6 there is a plot of distances squared, between the original m -adic representation, for $m = 10$, and the succession of best fits.

5.5 m -Adic Regression: Best Fit of Spectrometric Redshifts by Photometric Redshifts

From Table 1, we see that the binary representation, of spectroscopic and photometric redshifts, gives the best, closest correspondence. This is for all digits.

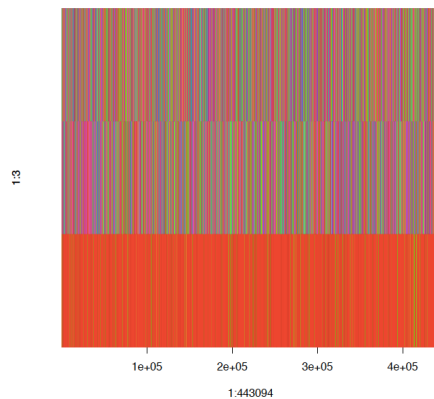


Figure 3: Spectroscopic redshifts. p -Adic display, for $p = 7$.

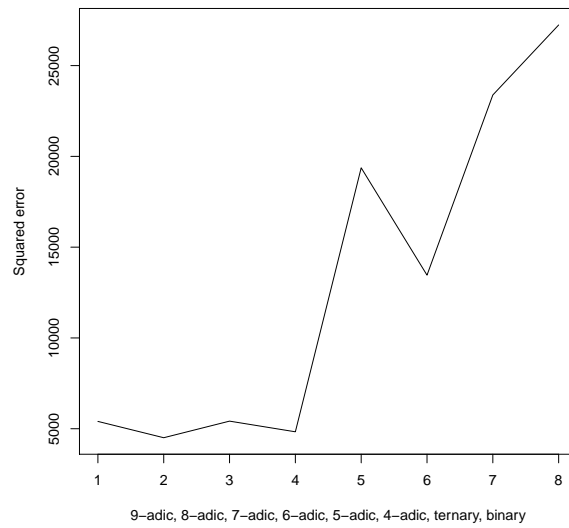


Figure 4: Spectroscopic redshifts. Squared distance, i.e. error, original 10-adic representation, and the sequence of m -adic best fits.

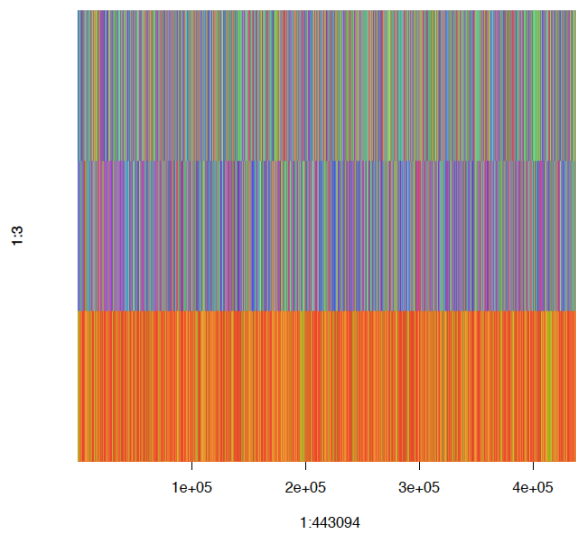


Figure 5: Photometric redshifts. Initial m -adic display, for $m = 10$. Three digits of precision used.

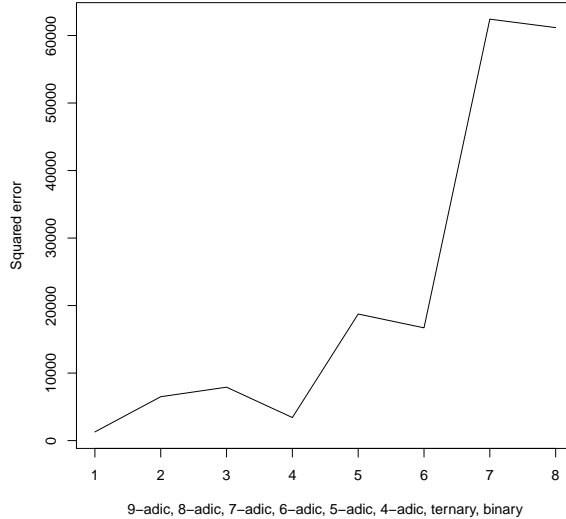


Figure 6: Photometric redshifts. Squared distance, i.e. error, original 10-adic representation, and the sequence of m-adic best fits.

Since we desire exact matching, as far as possible, rather than just such a real-valued degree of approximation, we look further for that objective.

In Table 2, it is seen that up to 57% of the digits in the ternary, or 3-adic, representations of spectroscopic and photometric redshifts, are identical. Let us see next, if this can be improved upon.

Table 3 displays the most successful outcome here. We are using just the first digit of the representation of redshifts, in m-adic representations, for $m = 10, 9, \dots, 3, 2$. We find that for the cases of either p-adic with $p = 5$, 5-adic, or m-adic with $m = 4$, we have 98% identity between spectroscopic and photometric redshifts. Thus, from this data set, comprising (SDSS, DR5, Stripe 82) redshifts for 443094 objects, the desired equivalence between spectroscopic and photometric redshifts, points to desirability of either 4-adic or 5-adic redshift encoding. These, respectively, comprise their values using the digit sets, 0, 1, 2, 3 and 0, 1, 2, 3, 4. Most of all in such representations, there are natural, implicit hierarchical data representations, i.e. here, regular 4-way and 5-way trees. If we were to accept a little less identity between the redshifts, to have just over 89% measurement identity, then we would be content with either of the ternary (p-adic with $p = 3$), or binary (p-adic with $p = 2$) representations.

Table 1: Totalled distance between spectroscopic and photometric redshifts

Representation	Distance
Original, m-adic	3497.347
m-adic, m = 9	3219.545
m-adic, m = 8	2960.628
p-adic, p = 7	2463.237
m-adic, m = 6	2102.937
p-adic, p = 5	1798.283
m-adic, m = 4	1401.31
p-adic, p = 3	1009.443
p-adic, p = 2	940.8114

Table 2: Identical digits between spectroscopic and photometric redshifts, the total number, and as the fraction of all digits in these 443094 objects.

Representation	No. identical digits	Fraction
Original, m-adic	508376	0.3824441
m-adic, m = 9	361332	0.2718249
m-adic, m = 8	404957	0.3046434
p-adic, p = 7	446470	0.3358731
m-adic, m = 6	487841	0.3669959
p-adic, p = 5	712084	0.5356907
m-adic, m = 4	745784	0.5610427
p-adic, p = 3	757357	0.5697489
p-adic, p = 2	736578	0.5541172

Table 3: Compared to Table 2, here just the first digit of precision is used. Identical digits between spectroscopic and photometric redshifts, the total number, and as the fraction of all digits in these 443094 objects.

Representation	No. identical digits	Fraction
Original, m-adic	366907	0.8280568
m-adic, m = 9	213872	0.4826786
m-adic, m = 8	247360	0.5582563
p-adic, p = 7	262474	0.5923664
m-adic, m = 6	262474	0.5923664
p-adic, p = 5	434736	0.9811372
m-adic, m = 4	434736	0.9811372
p-adic, p = 3	395490	0.8925646
p-adic, p = 2	395490	0.8925646

6 Conclusions

It is acknowledged that the experimental work here has only used a training set in order to specify a model for matching based on number representation. If used for regression, it is seen to be a method of cluster-wise regression, generalizing nearest neighbour regression. The clustering or binning of the data values has a central role in this methodology.

Precision of measurement is a statistical issue, that was so fundamental to the seminal work of Carl Friedrich Gauss. In this work, our focus has been on clustering, or binning, or interval specification. For real valued data, this is an approach to replacing a range of values, in an interval, with a cluster label, e.g. $x + \epsilon \rightarrow c$ with $x, \epsilon \in \mathbb{R}, c \in \mathbb{Z}_+$.

Longer term, our objective is more to do with tracking, and in a non-statistical sense, inferring structure from the data. Such structure includes relative distance from the observer, and associated with this, inter- and intra-distances for clustered objects. Central to this is the topology rather than geometry manifested by observed (spatial, shaped, ordered) data. Another, longer term goal, is the explicit incorporation of the time dimension.

Extending this methodology is additionally of interest, as written in [9], “Clearly those interested in (re)structuring data for any purpose ought to keep a close watch for innovative and interesting approaches in the cosmological simulation field in the future!”. This continues: “However, the structuring of particles with a view towards force calculations has also something to learn from experience in the cluster analysis field.”

Finally, of note, is the potential to relate this work (in a manner, to be determined) with the p-adic and adelic number theoretical explanations of dark matter and dark energy, [6]. In [13], there is some further discussion of this. In [6], a section heading is as follows (p. 40): “Adelic Universe with Real and p-Adic Worlds”, and there is this motivation (p. 26): “Let us use terms real and p-adic to denote those aspects of the universe which can be naturally described by real and p-adic numbers, respectively. We conjecture here that the visible and dark sides of the universe are real and p-adic ones, respectively.”

In the different context of social science, [12] considers hierarchical representation of extent and degree of change in multivariate time series. The aim is to uncover relationships between social violence and market forces. There also, internal structure arising from inherent heterogeneity in our data is directly used.

Acknowledgement

The SDSS data were provided by Raffaele D’Abrusco and Giuseppe Longo.

References

- [1] Adelman-McCarthy, J.K. et al. 2007, *ApJ Supplement Series*, 172 (2), 634

- [2] Bolton, A.S., Schlegel, D.J., Aubourg, É., Bailey, S., Bhardwaj, V., Brownstein, J.R., Burles, S., Chen, Y.-M., Dawson, K., Eisenstein, D.J., Gunn, J.E., Knapp, G.R., Loomis, C.P., Lupton, R.H., Maraston, G., Muna, D., Myers, A.D., Olmstead, M.D., Padmanabhan, N., Pâris, I., Percival, W.J., Petitjean, P., Rockosi, C.M., Ross, N.P., Schneider, D.P., Shu, Y., Strauss, M.A., Thomas, D., Tremonti, C.A., Wake, D.A., Weaver, B.A., Wood-Vasey, W.M. 2012, *AJ*, 144, 144
- [3] Csabai, I., Budavari, T., Connolly, A.J., Szalay, A.S., Gyory, Z., Benitez, N., Annis, J., Brinkmann, J., Eisenstein, D., Fukugita, M., Gunn, J., Kent, S., Lupton, R., Nichol, R.C., Stoughton, C. 2003, *AJ*, 125, 580 (<http://arxiv.org/abs/astro-ph/0211080>, 5 Nov. 2002)
- [4] d'Abrusco, R., Longo, G., Paolillo, M., Brescia, M., De Filippis, E., Staiano, A., Tagliaferri, R. 2006, “The use of neural networks to probe the structure of the nearby universe”, *Proc. ADA-4: Astronomical Data Analysis IV* (Sept. 2006, Marseilles), p. 79 (arXiv:astro-ph/0701137v1, 5. Jan. 2007)
- [5] d'Abrusco, R., Staiano, A., Longo, G., Brescia, M., Paolillo, M., De Filippis, E., Tagliaferri, R. 2007, *ApJ*, 663, 752 (<https://arxiv.org/abs/astro-ph/0703108>)
- [6] Dragovich, B. 2006, “p-Adic and adelic cosmology: p-Adic origin of dark energy and dark matter”, *Proc. 2nd International Conference on p-Adic Mathematical Physics*. (arXiv:hep-th/0602044v1, 4 Feb. 2006)
- [7] Firth, A.E., Lahav, O., Somerville, R.S. 2003, *MNRAS*, 339, 1195
- [8] Khrennikov, A., Oleshko, K., de Jesús Correa López, M. 2016, “Modeling fluid’s dynamics with master equations in ultrametric spaces representing the treelike structure of network of capillaries”, *Entropy*, 18 (7), 249
- [9] Murtagh, F. 1988, *Computer Physics Communications*, 52, 15
- [10] Murtagh, F., Raftery, A.E., Starck, J.L. 2005, “Bayesian inference for multiband image segmentation via model-based cluster trees”, *Image & Vision Computing*, 23, 587
- [11] Murtagh, F. 2016, “Sparse p-adic data coding for computationally efficient and effective big data analytics”, *p-Adic Numbers, Ultrametric Analysis and Applications*, 8 (3), 236
- [12] Murtagh, F., Spagat, M., Restrepo, J.A. 2011, “Ultrametric wavelet regression of multivariate time series: application to Colombian conflict analysis”, *IEEE Transactions on Systems, Man, and Cybernetics–Part A: Systems and Humans*, 41, 254
- [13] Murtagh, F. 2017, *Data Science Foundations: Geometry and Topology of Complex Hierarchic Systems and Big Data Analytics*, Chapman and Hall, CRC Press (Taylor and Francis), Boca Raton, FL, forthcoming.

- [14] Shu, Y., Bolton, A.S., Schlegel, D.J., Dawson, K.S., Wake, D.A., Brownstein, J.R., Brinkmann, J., Weaver, B.A. 2012, *AJ*, 134, 90
- [15] Stripe 82 2016, *Images Tutorial*, http://www.sdss.org/dr12/tutorials/get_stripe82_images/
- [16] Vanzella, E., Cristiani, S., Fontana, A., Nonino, M., Arnouts, S., Giallongo, E., Grazian, A., Fasano, G., Popesso, P., Saracco, P., Zaggia, S. 2004, *A&A*, 423, 761 (arXiv:astroph/0312064v1, 2 Dec. 2003)